

Chapter 3

Nuclear Models

3.1 Introduction

The study of complex many-body quantum systems like atomic nuclei poses several challenges. Moreover, the nature of the short-range nuclear force that binds nucleons in a nucleus is in contrast to those of long-range forces such as electromagnetic or gravitational forces. In order to study and understand the physics behind such a complex system, it is always wise to propose a simplified but mathematically solvable theory which should contain sufficient physical insight into the subject. This leads to the development of *nuclear models* with a view to account for already observed nuclear phenomena as well as to predict the properties which are yet to be measured.

3.2 Liquid Drop Model

George Gamow and Neils Bohr were among the first persons to propose a liquid drop model for atomic nuclei [49, 86]. The model describes the nucleus macroscopically. A nucleus is considered as a drop of incompressible liquid, and the molecules constituting the liquid drop are considered to be analogous to the nucleons in a nucleus. Such analogies between

a liquid drop and a nucleus is really interesting. Starting from the fact that the density of a liquid is almost independent of its size, to the proportionality of energy required for evaporating a drop into well-separated molecules are some of the examples which show similarity between the two systems. Moreover, inspired by the observation of saturation of nuclear forces (constant binding energy per nucleon (~ 8.5 MeV)) as a function of the mass number A , Bethe and Weizsäcker [87] proposed the *semi-empirical mass formula* to reproduce the afore mentioned behavior of binding energy (E_B) per nucleon :

$$E_B = a_v A - a_s A^{2/3} - a_c \frac{Z^2}{A^{1/3}} - a_a \frac{(N-Z)^2}{A} + \delta_p. \quad (3.1)$$

where the first term corresponds to the volume energy, followed by the surface term. The third term incorporates the Coulomb energy which is dependent on the atomic number Z of the nucleus. The effect of asymmetric distribution of protons (Z) and neutrons (N) is incorporated in by the penultimate term. The last term takes care of the pairing energy to account for the more stable nucleus with paired protons and neutrons. The pairing term has the following form:

$$\delta_p = \begin{cases} +a_p \frac{1}{A^{3/4}}, & \text{even - even nucleus} \\ 0, & \text{odd - even or even - odd nucleus} \\ -a_p \frac{1}{A^{3/4}}, & \text{odd- odd nucleus.} \end{cases} \quad (3.2)$$

The corresponding coefficients to each of the above terms are a_v , a_s , a_c , a_a and a_p , respectively. An estimate of values of coefficients is given by Green [88].

$$\begin{aligned} a_v &= 15.75 \text{ MeV}, a_s = 17.8 \text{ MeV}, a_c = 0.71 \text{ MeV}, \\ a_a &= 23.70 \text{ MeV}, a_p = 33.5 \text{ MeV}. \end{aligned} \quad (3.3)$$

The liquid drop model was successful in explaining the bulk properties of the nucleus, such as mass, binding energy etc. Moreover, Bohr and Wheeler were motivated to apply the same hypothesis to explain the fission process [89]. However, the model fails to describe some of the microscopic properties. As an example, this model fails to reproduce observed magic numbers. To counter the unanswered features in a nuclear shell model was proposed by Myer and janssen, which is discussed in the next section.

3.3 Shell Model

3.3.1 Spherical shell model

Motivated with the clarification of complexities in atomic structure, with the help of atomic theory based on shell structure model, physicists made an attempt to apply similar model for studying nuclear structural properties with a hope to explain extra stability of certain nuclei with nucleon numbers equal to the magic number (2, 8, 20, 28, 50, 82 and 126) [90] [see Fig. 3.1]. The model in its simplest form, assumes the independent motion of a single nucleon governed by a mean field potential developed by all the surrounding nucleons. Nucleons being Fermions, the Pauli exclusion principle is applicable. The shell model was independently proposed by Mayer [91] and Haxel *et al.* [3] in 1949.

The simplest form of the shell model Hamiltonian is:

$$\mathcal{H} = \sum_{i=1}^A -\frac{\hbar^2}{2m} \nabla_i^2 + \frac{1}{2} \sum_{i,j=1}^A V_{i,j}. \quad (3.4)$$

where $V_{i,j}$ is the two body interaction term. The Hamiltonian can, in turn, be rewritten in terms of an average one-body interaction term $U(r_i)$, i.e.

$$\mathcal{H} = \sum_{i=1}^A \left[-\frac{\hbar^2}{2m} \nabla_i^2 + U(r_i) \right] + \left[\frac{1}{2} \sum_{i,j=1}^A V_{i,j} - U(r_i) \right] = \mathcal{H}_0 + \mathcal{H}_{res}. \quad (3.5)$$

Osc. No.	Square well	Spect. term	Spin term	No. of states	Shells	Total No.		
0	1s	1s	1s _{1/2}	2	2	2		
1	1p	2p	1p _{1/2}	2	6	8		
			1p _{3/2}	2				
2	1d	3d	1d _{3/2}	6	12	20		
			1d _{5/2}	4				
			2s	2s			2s _{1/2}	2
3	1f	4f	1f _{7/2}	8	22	28?		
			1f _{5/2}	6				
			2p _{3/2}	4				
			2p _{1/2}	2				
			1g _{9/2}	10			50	
4	1g	5g	1g _{7/2}	8	32	82		
			2d _{5/2}	6				
			2d _{3/2}	4				
			3s	3s			3s _{1/2}	2
5	1h	6h	1h _{11/2}	12	44	126		
			1h _{9/2}	10				
			2f _{7/2}	8				
			2f _{5/2}	6				
			3p _{3/2}	4				
			3p _{1/2}	2				
6	1i	7i	1i _{13/2}	14	44	126		
			1i _{11/2}	12				
			2g	6g			2g _{7/2}	8
			3d	5d			3d _{5/2}	6
6	4s	4s	4s	2	2	2		
			4s	2				

Figure 3.1 Single particle energy levels for square-well potential alongwith the inclusion of anharmonic term as well as spin orbit coupling [91].

where \mathcal{H}_0 is the one body part of the Hamiltonian which describes the motion of A nucleons in the average potential $U(r_i)$ whereas \mathcal{H}_{res} contains the two body “residual interaction” terms. The simplest form of the mean-field potential is described by a simple harmonic oscillator potential but the actual potential lies somewhere between simple harmonic oscillator and the square-well potential. If a spherically symmetric harmonic oscillator

potential is of the form $V_{ho} = \frac{1}{2}m\omega_0^2(r^2 - R_0^2)$, where R_0 is the mean radius, is used as the mean potential, then the shell energy eigenvalues come out to be :

$$E_{ho} = (N_q + 3/2)\hbar\omega. \quad (3.6)$$

where N_q is the *principal quantum number* which is defined in terms of radial quantum number n and azimuthal quantum number l such that $N_q = 2(n - 1) + l$. The most extensively used potential is the 'Woods Saxon' potential which is given as follows :

$$V_{ws}(r) = -\frac{V_{ws0}}{1 + \exp[(r - R_0)/a_{sk}]}. \quad (3.7)$$

where the parameters R_0 and a_{sk} correspond to the mean radius ($\sim 1.2A^{1/3}$) and skin thickness ($\approx 0.5 fm$), respectively. The depth of the well, V_{ws0} , with a value $\approx 50 MeV$ is adjusted to give proper separation energy. However, even though the above-mentioned potentials are capable of explaining lower magic numbers, say up to 20, but higher magic numbers are not produced in calculations. Finally, the success was achieved with the inclusion of the spin-orbit coupling term into the given mean potentials. The spin-orbit interaction can be written as $f(r)\mathbf{l}\cdot\mathbf{s}$. The expectation value of $\mathbf{l}\cdot\mathbf{s}$ is given in terms of expectation values of total angular momentum \mathbf{I} , orbital angular momentum \mathbf{l} and spin quantum number s :

$$-\langle \mathbf{l}\cdot\mathbf{s} \rangle = \frac{1}{2}[l(l+1) + s(s+1) - j(j+1)]\hbar^2. \quad (3.8)$$

The $\mathbf{l}\cdot\mathbf{s}$ term lifts the degeneracy in $j = l \pm 1/2$ levels by discriminating between the nucleons on the basis of whether the spin angular momentum of a nucleon is aligned or antialigned with the orbital angular momentum. The splitting energy is $\Delta E \propto 2l+1$. The shell model was successful in explaining the magic numbers, ground state nuclear spins, energy levels, magnetic moments, etc. [92, 93].

3.3.2 Deformed Shell Model

The spherical shell model is based on a spherically symmetric potential. In the year 1955, Nilsson [94] proposed to use a deformed potential in order to address the physical properties of nuclei far from closed shells. In a deformed nucleus, \mathbf{j} is no longer a good quantum number. Moreover, the observed degeneracy corresponds to $(2j+1)$ orientations across a specific single particle state with total angular momentum value j . The nucleus still preserves the reflection symmetry. As a result, if the component of j is denoted by Ω , $\pm\Omega$ projections attain the same energy eigenvalue. Assuming the axial symmetry of the nucleus about the z -axis, the Hamiltonian for the three-dimensional harmonic oscillator can be written in the form

$$\mathcal{H}_{sp} = -\frac{\hbar^2}{2m}\nabla^2 + \frac{1}{2}m[\omega_x^2 x^2 + \omega_y^2 y^2 + \omega_z^2 z^2]. \quad (3.9)$$

The eigenenergy states will be

$$E(n_x, n_y, n_z) = \hbar\omega_x(n_x + \frac{1}{2}) + \hbar\omega_y(n_y + \frac{1}{2}) + \hbar\omega_z(n_z + \frac{1}{2}) = \hbar\omega_{\perp}(n_x + n_y + 1) + \hbar\omega(n_z + \frac{1}{2}). \quad (3.10)$$

where the angular frequencies along the x and y , coordinates are equal, thus, i.e., $\omega_x = \omega_y = \omega_{\perp}$ and $\omega = \omega_z$. Now the total quantum number N_q can be written as a combination of n_x , n_y , and n_z .

$$N_q = (n_x + n_y) + n_z = n_{\perp} + n_z. \quad (3.11)$$

Therefore, each single particle eigenstate can be designated by three quantum numbers (N, n_z, Λ) , where Λ is the projection of orbital angular momentum on the symmetry axis. Furthermore, when the projection of spin quantum number along the symmetry axis is

considered to be $\Sigma = \pm \frac{1}{2}$, then the projection of total angular momentum is given by $\Omega = \Lambda + \Sigma$. Hence, the eigenstates are characterized by $[N, n_z, \Lambda]\Omega$.

Similar to the spherical case, it was found to be necessary to include the spin-orbit coupling term and an anharmonic term to yield the correct sequence of levels. Thus, the so-called Nilsson Hamiltonian takes the form:

$$\mathcal{H} = -\frac{\hbar^2}{2m}\nabla^2 + \frac{1}{2}M[\omega_{\perp}^2(x^2 + y^2) + \omega_z^2 z^2] + C\mathbf{l}\cdot\mathbf{s} + D\mathbf{l}^2. \quad (3.12)$$

where C and D are constants in spin-orbit and anharmonic terms, respectively. The angular frequencies ω_x and ω_z are written in terms of a constant frequency ω_0 and adjusted quadrupole deformation parameter ε_2 .

$$\omega_{\perp}^2 = \omega_0^2(1 + \frac{2}{3}\varepsilon_2). \quad (3.13)$$

$$\omega_z^2 = \omega_0^2(1 - \frac{4}{3}\varepsilon_2). \quad (3.14)$$

In order to conserve the nuclear volume with a change in deformation, the following condition should remain valid :

$$\omega_x^2 \omega_y^2 \omega_z^2 = \text{constant}, \quad (3.15)$$

$$\omega_x^2 \omega_y^2 \omega_z^2 = \omega_0^6(1 + \frac{2}{3}\varepsilon_2)^2(1 - \frac{4}{3}\varepsilon_2), \quad (3.16)$$

$$\omega_0(1 - \frac{4}{3}\varepsilon_2 - \frac{16}{27}\varepsilon_3)^{1/6} = \text{constant}. \quad (3.17)$$

Substituting equations (3.13 - 3.17) into (3.12) we obtain :

$$\mathcal{H} = -\frac{\hbar^2}{2m}\nabla^2 + \frac{1}{2}m\omega_0^2 r^2 - m\omega_0^2 r^2 \varepsilon_2 \frac{4}{3} \sqrt{\frac{\pi}{5}} Y_{20}(\theta, \phi) + C\mathbf{l}\cdot\mathbf{s} + D\mathbf{l}^2. \quad (3.18)$$

It can be easily realized that the Hamiltonian with deformed potential differs from the spherically-symmetric shell model Hamiltonian by a perturbative factor of

$$\mathcal{H}_{pert} = m\omega_0^2 r^2 - m\omega_0^2 r^2 \varepsilon_2 \frac{4}{3} \sqrt{\frac{\pi}{5}} Y_{20}(\theta, \phi). \quad (3.19)$$

Thus, the energy shift due to perturbation in spherically symmetric potential can easily be calculated by applying the virial theorem, the ‘‘Wigner-Eckart’’ theorem and angular momentum algebra. It is also evident that the equation 3.18 violates the isospin symmetry. It is dependent on the type of nucleon. The concept is manifested by introducing two new parameters in equation 3.12. The two constants C and D are defined in terms of κ and μ such that $\kappa = C/2\hbar\omega_0$ and $\mu = 2D/C$. These parameters are derived for different nuclear mass regions by fitting the observed energy levels. The equation 3.18 can be worked out for protons and neutrons separately with solutions similar to those shown in Fig. 3.2.

There is an alternative approach of using cylindrical coordinates to solve the Hamiltonian in order to avoid the coupling between N and $N \pm 2$ energy states [95]. Moreover, given the fact that the system under consideration is axially symmetric, the cylindrical representation of the coordinate frame proves to be advantageous.

3.3.3 Strutinsky Shell Correction

As seen in section 3.2, various bulk properties of a nucleus can be addressed using the liquid drop model which assumes that the nucleons are uniformly distributed in phase space, thus ignoring the nuclear shell effect completely if any. In order to account for the fluctuations in the actual distribution of single-particle levels relative to a smooth distribution of levels, Strutinsky came up with the idea of a shell correction procedure [97]. The correction incorporates nuclear shell and other quantum effects as a small deviation from the uniform distribution of energy levels in the liquid drop model. In the

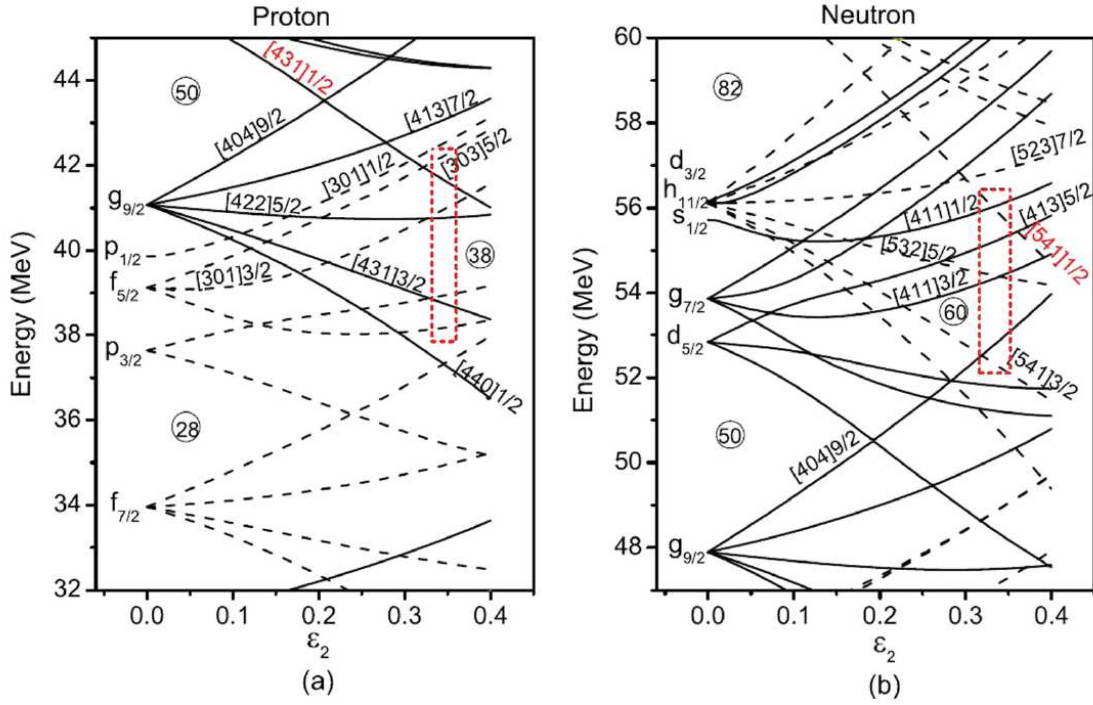


Figure 3.2 Nilsson diagram showing proton and neutron single-particle energies with the shell closure (a) $28 < Z < 50$ (b) $50 < N < 82$ as a function of deformation parameter ϵ_2 . Figure taken from Ref. [96].

Nilsson model, the average behavior of nuclear deformation energy was considered to be proportional to the single-particle energies ϵ_q of the lowest occupied levels :

$$E(def) = \sum_{q=1}^A \epsilon_q. \quad (3.20)$$

However, experimental observation reveals a discrete, unequally spaced energy spectrum away from the Fermi surface region. Thus, to counterbalance the discrepancy, the average energy part in the Nilsson model was upgraded as

$$E_{(total)} = E_{LDM} + \delta E_p(def) + \delta E_n(def). \quad (3.21)$$

where δE_p and δE_n are the shell correction energies for protons and neutrons, respectively, as both types of nucleons occupy the shells in an independent way. The correction terms are derived from the difference of the total deformation energy and its average.

3.4 Collective Behavior

The large ground state quadrupole moments, enhanced $E2$ transition rates, energy spectrum with 'rotor-like' behavior, etc., are some of the characteristics which indicate that rather than single particle behavior, coherent contribution from all nucleons might be prevalent in nuclei away from shell closure. Collective behavior of nuclei was studied in the framework of *collective model* developed by A. Bohr and B. R. Mottleson [98–100]. The shape of a deformed nucleus, in the vibrational limit, can be described in terms of the deformed instantaneous radius vector $R(\theta, \phi, t)$ as

$$R(\theta, \phi, t) = R_{sp} \left[1 + \sum_{\lambda=0}^{\infty} \sum_{\mu=-\lambda}^{\lambda} \alpha_{\lambda\mu}(t) Y_{\lambda\mu}(\theta, \phi) \right]. \quad (3.22)$$

where R_{sp} is the radius of spherical nucleus. The above equation shows the dependence of $R(\theta, \phi, t)$ on spherical harmonics $Y_{\lambda\mu}(\theta, \phi)$ mediated by *collective coordinates* $\alpha_{\lambda\mu}$. The parameter λ describes the multipolarity of nuclear shape oscillations while μ is the corresponding projection of λ . The monopole mode $\lambda = 0$ with non-zero α_{00} allows only a change in nuclear radius. Based upon the argument that the nucleus is incompressible, the monopole term can be discarded. The dipole vibration is described by the term $\lambda = 1$ which signifies the net displacement of the center of mass of the nucleus. The term can be reduced to zero by choosing a reference frame with its origin coinciding with the center of mass of the system, i.e. by *translational symmetry*. The term with $\lambda = 2$ is associated with the nuclear quadrupole deformation which is dominant in low energy excitations. With the choice of body-fixed axis coinciding with the principal axis, the five coefficients $\alpha_{2\mu}$

actually get reduced to two independent parameters α_{20} and $\alpha_{22} = \alpha_{2-2}$. Now, following the Lund convention [101] these parameters can be transformed in terms of Hill-Wheeler coordinates [102]:

$$\alpha_{20} = \beta \cos \gamma, \alpha_{22} = \frac{\beta}{\sqrt{2}} \sin \gamma. \quad (3.23)$$

where the parameters β and γ are the axial and triaxiality deformation parameters. The equation 3.22 can be rewritten for quadrupole deformation in the following form :

$$R(\theta, \phi) = R_{sp} \left[1 + \beta \sqrt{\frac{5}{16\pi}} (\cos \gamma (\cos^2 \theta - 1) + \sqrt{3} \sin \gamma \sin^2 \theta \cos 2\phi) \right]. \quad (3.24)$$

Deviation from the radius of spherical nucleus along the three coordinate axes is respectively given by

$$\Delta R_k = R(\theta, \phi) - R_{sp} = R_{sp} \sqrt{\frac{5}{4\pi}} \beta \left(\cos \left(\gamma - \frac{2\pi}{3} k \right) \right). \quad (3.25)$$

where k defines the coordinate axis number; 1, 2, 3. For axially symmetric deformation with $\gamma = 0$, axial deformation parameter can be derived from equation 3.25 :

$$\beta = \frac{4}{3} \sqrt{\frac{\pi}{5}} \frac{\Delta R_{3-1}}{R_{sp}}. \quad (3.26)$$

When $\beta > 0$, the nucleus is a *prolate ellipsoid* whereas the nucleus is observed to attain *oblate ellipsoid* shape with $\beta < 0$. Another parameter which is most often used to describe the axial deformation is ε_2 , which can be associated with β such that

$$\varepsilon_2 = \frac{3}{4} \sqrt{\frac{5}{\pi}} \beta \approx 0.95\beta. \quad (3.27)$$

Furthermore, a nucleus spans the entire region of polar plot in $\beta - \gamma$ plane with different shapes at different orientations.

- Prolate : $\gamma = 0^\circ, 120^\circ, 240^\circ$

- Oblate : $\gamma = 60^\circ, 120^\circ, 300^\circ$

Now coming to the next higher mode, i.e., $\lambda = 3$. The mode corresponds to octupole deformation thereby producing triaxial shaped or *pear shaped* nucleus which does not obey the reflection symmetry. The contribution from higher order modes is quite feeble and less useful information can be obtained from such studies.

3.4.1 Cranking Model

The model which was first proposed by Inglis as the *cranking model* [103, 104], includes the rotational description in nuclei and quantum mechanical independent-particle model description of a nucleus. The model was further improved by Bengtsson and Frauendorf [105–107]. The straightforward process to study the properties of a rotating nucleus is to compel it to rotate with a certain fixed frequency or to “crank”. A body-fixed coordinate system having a fixed orientation relative to the lab frame can be considered. Thus, the reference system rotates with a fixed frequency, say, ω with respect to the laboratory-fixed frame of reference. Fig. 3.3 displays the two types of coordinate systems, each is related to the other through rotational transformation equations (the primed coordinates being the rotating body-fixed coordinate system):

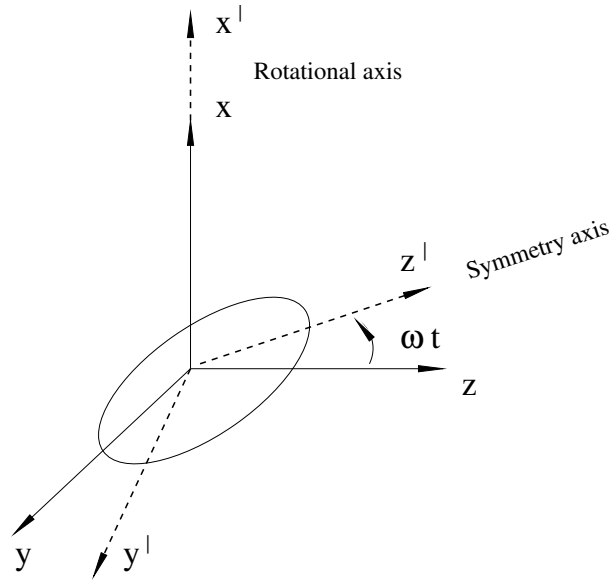


Figure 3.3 Rotating body-fixed coordinate system (shown with primed coordinates) with respect to laboratory frame of reference.

$$x' = x \quad (3.28)$$

$$y' = y \cos \omega t + z \sin \omega t \quad (3.29)$$

$$z' = -y \sin \omega t + z \cos \omega t \quad (3.30)$$

The final form of cranking Hamiltonian H_ω of the system rotating with ω frequency around, say, x_1 axis will be :

$$H_\omega = H_0 + \omega I'_x \quad (3.31)$$

The second term which contains the combined effect of Coriolis and centrifugal forces [40], is responsible for modifying the nucleonic orbits. The Coriolis factor is responsible for aligning the angular momentum of nucleons along the rotational axis. Moreover, effect of Coriolis force varies according to the strength of the force, i.e, whether Coriolis force

can be considered as a small perturbation or it is the sole dominant factor in the equation of motion [108, 109]. The cranking Hamiltonian remains invariant under rotation with respect to rotation about z -axis.

3.4.2 Nuclear Rotation

The rotation of a nucleus can be of two types; (a) rotation around the symmetry axis where the symmetry and the rotation axis coincides and (b) rotation around an axis perpendicular to the symmetry axis.

Rotation around the symmetry axis

In a rotation-symmetric potential, the eigenfunctions of non-rotating single-particle potential commutes with the projection of angular momentum on symmetry axis, say, z -axis. The eigenvalue equation for the rotating Hamiltonian

$$H_\omega = H_0 - \omega I_z, \quad (3.32)$$

can be written as

$$e_i^\omega = e_i - \omega \Omega_z. \quad (3.33)$$

Ω_z is the projection of angular momentum along the symmetry axis (sometimes referred to as m_i). The e_i^ω s are the single-particle Routhians. The equation 3.33 clearly shows a linear characteristics of Routhians with respect to angular frequency. The slope of the curve determines the angular momentum projection. The total energy of the system with A number of nucleons can be determined by summing up energy of the all the nucleons occupying states up to Fermi level. Thus, the states generated with the rotation around the symmetry axis are mostly the optimal states along the Fermi surface. Non-optimal states

can be explained on the basis of particle-hole excitations which are based on optimal states. Hence, this non-collective rotation does not result in the formation of rotational bands; rather, only pure single-particle configurations are obtained. These configurations are estimated on $(e_i - m_i)$ plane through the slope of tilted Fermi surface which is proportional to ω [101, 110]. An example is shown in Fig. 3.4. The figure illustrates how a couple of extra protons outside the ^{90}Zr core in ^{93}Nb can be arranged to define Fermi surfaces (shown with blue colored straight lines).

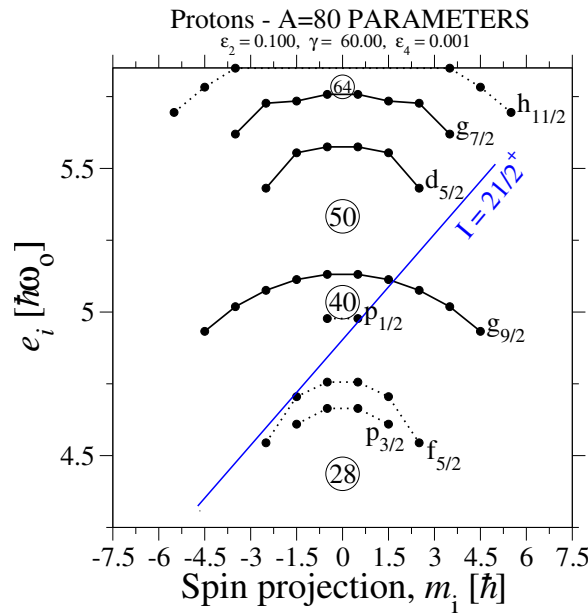


Figure 3.4 Single-particle energies as a function of spin projection for rotation around symmetry axis. The Figure taken from Ref. [111].

Rotation Perpendicular to the Symmetry Axis

Let the symmetry axis be the z -axis, but let us consider the axis of rotation to be x -axis. The substantial change in cranking Hamiltonian will be due to change in total angular momentum along x -axis rather than z -axis as in the previous case.

$$H_\omega = H_0 - \omega I_x. \quad (3.34)$$

Unlike the last situation, Ω_x no longer remains a good quantum number for non-rotated single-particle Hamiltonian. Thus, it is necessary to look for new symmetries which will remain conserved under this type of rotation. One such example of symmetry is parity which defines space reflection symmetry. The other one is signature quantum number (α), which is defined as :

$$R_x(\pi)\psi_\alpha = \exp(-i\pi j_x)\psi_\alpha = \exp(-i\pi\alpha)\psi_\alpha. \quad (3.35)$$

where $R_x(\pi)$ is the rotation operator and ψ_α is the wavefunction with signature α . The signature quantum number determines nuclear properties under a rotation of π around the rotational axis. The signature α can have two values $\alpha = \frac{1}{2}$ and $-\frac{1}{2}$ for a single particle system. This shows that unlike the non-rotating potential, where degeneracy prevails in time-reversed states with spin projections Ω and $-\Omega$, during rotation, a state can be designated as a linear combination of $\alpha = \frac{1}{2}$ and $\alpha = -\frac{1}{2}$, respectively. The signature can be defined in another way as the eigenvalue of the rotation operator, i.e. $r = \exp(-i\pi\alpha)$. The additive property of α makes it convenient to handle the mathematical equations and, thus, the following relations between r and α follow:

For an even numbered particle system

$$r = +1(\alpha = 0)I = 0, 2, 4, \dots, \quad (3.36)$$

$$r = -1(\alpha = 1)I = 1, 3, 5, \dots \quad (3.37)$$

whereas for the system having odd number of particles

$$r = -i(\alpha = \frac{1}{2})I = \frac{1}{2}, \frac{5}{2}, \frac{9}{2}, \dots, \quad (3.38)$$

$$r = +i(\alpha = -\frac{1}{2})I = \frac{3}{2}, \frac{7}{2}, \frac{11}{2}, \dots \quad (3.39)$$

The equations can be combined into one equation:

$$I = \alpha \text{mod} 2. \quad (3.40)$$

Finally, the eigenvalue of H_ω can be given as:

$$E_\omega = \langle |H_0| \rangle - \omega \langle |I_x| \rangle. \quad (3.41)$$

3.4.3 cranked Nilsson Strutinsky Model

Cranking model provides a microscopic description of rotating nuclei with the total angular momentum being equal to the sum of angular momenta from individual particles. Thus, collective and non-collective rotations can be studied on the same footing. Given these advantages, the model also has some demerits. The Cranking Model is based on a semiclassical approach where rotation is imposed on the system externally. The model uses a fixed rotation axis resulting in the breaking of rotational invariance. Moreover, the wavefunctions calculated using the model are not eigenstates of the angular momentum operator which can pose difficulty in cases of calculating electromagnetic transition probabilities. Moreover, the interaction between different bands takes place at a specific ω instead of specific I . Poor approximation for weakly crossing bands, associated with large fluctuations in $\langle j_x \rangle$ is another shortcoming of the model. The anomaly arises because the model assumes constant fluctuation in $\langle j_x \rangle$ at crossing [112]. In order to overcome the above shortcomings, configuration dependent cranked Nilsson Strutinsky (CNS) approach was proposed [113–117]. The model is based on Nilsson potential while incorporating the rotational mechanism and Strutinsky shell corrections within it. The advantage of the Nilsson potential is that it is quite successful in identifying configurations compared to other models. The designation of configurations can be done on the basis of particles in specified orbitals with parity and signature as good quantum numbers

and by particles in different N_{rot} - shells [112]. The total nuclear energy E_{tot} at specific deformation $\bar{\epsilon} \cong (\epsilon_2, \gamma, \epsilon_4)$ and a specific spin, say I_0 is given by

$$E_{tot}(\bar{\epsilon}, I_0) = E_{LD}(\bar{\epsilon}, I = 0) + \frac{1}{2J_{rig}(\bar{\epsilon})} I_0^2 + E_{sh}(\bar{\epsilon}, I_0). \quad (3.42)$$

where, first two terms constitute the rotating liquid drop energy. The rigid body moments of inertia are calculated with a radius parameter $r_0 = 1.16$ fm and a diffuseness of $a = 0.6$ fm [117]. The static liquid drop energy was calculated by Pomorsky and Dudek [118–120] by using Lublin-Strasbourg Drop model (LSD).

$$\begin{aligned} E_{LD}(\bar{\epsilon}, I = 0) = & -a_v(1 - k_v T^2)A - a_s(1 - k_s T^2)A^{2/3}B_s(\bar{\epsilon}) - \frac{3}{5} \frac{e^2 Z^2}{1.2160 * A^{1/3}} B_c(\bar{\epsilon}) \\ & + C_4 \frac{Z^2}{A} - b_{cur}(1 - k_{cur} T^2)A^{1/3} B_{cur}(\bar{\epsilon}) - E_{cong}. \end{aligned} \quad (3.43)$$

where, $B_s(\bar{\epsilon}) = E_s(\bar{\epsilon})/E_s(\bar{\epsilon} = 0)$, $B_c(\bar{\epsilon}) = E_c(\bar{\epsilon})/E_c(\bar{\epsilon} = 0)$, and $B_{cur}(\bar{\epsilon}) = E_{cur}(\bar{\epsilon})/E_{cur}(\bar{\epsilon} = 0)$ are the surface, Coulomb, and curvature energy terms, respectively, of a nucleus with a sharp surface in units of their corresponding values for a spherical nucleus. E_{cong} is the congruence energy which is equal to $-10 \text{ MeV} \exp(-42|T|/10)$. $T = \frac{N-Z}{A}$ denotes the isospin factor. The fourth term accounts for the correction in Coulomb energy due to surface diffusion of the charge distribution [112, 118–120]. Parameters for the LSD model given below were obtained by fitting the experimental binding energies [118]:

$$a_v = -15.4920 \text{ MeV}, k_v = 1.8601, \quad (3.44)$$

$$a_s = 16.9707 \text{ MeV}, k_s = 2.2938, \quad (3.45)$$

$$C_4 = 0.9181 \text{ MeV}, \quad (3.46)$$

$$b_{cur} = 3.8604 \text{ MeV}, k_{cur} = -2.3764. \quad (3.47)$$

In the equation, the last term corresponds to the difference between discrete and smoothed (shown with \sim) single-particle energy sums, known as shell energy and is defined as :

$$E_{sh}(\bar{\epsilon}, I=0) = \sum e_i(\omega, \bar{\epsilon}) |_{I=I_0} - \sum \widetilde{e_i(\tilde{\omega}, \bar{\epsilon})} |_{\tilde{I}=I_0}. \quad (3.48)$$

where, both the energy expressions are solved at different frequencies. The smoothed energy term is parameterized as

$$\sum \widetilde{e_i(\tilde{\omega}, \bar{\epsilon})} |_{\tilde{I}=I_0} = E_0 + \frac{1}{2J_{str}(\bar{\epsilon})} I_0^2 + bI_0^4, \quad (3.49)$$

where, $J_{str}(\bar{\epsilon})$ is the Strutinsky smoothed moment of inertia and $E_0 = \sum \widetilde{e_i(\tilde{\omega}, \bar{\epsilon})} |_{\tilde{I}=0}$. The value of constant b remains insignificant for lighter nuclei. The values of all the constants are determined by calculating smoothed sum at different frequencies [121].

The cranked single-particle Nilsson Hamiltonian would have following form :

$$H_\omega = H_{ho}(\epsilon_2, \gamma) + 2\hbar\omega_0\rho^2\epsilon_4V_4(\gamma) + V' - \omega j_x. \quad (3.50)$$

where $H_{ho}(\epsilon_2, \gamma)$ is the deformed harmonic oscillator potential and ρ is the radius in stretched coordinate system. Hexadecapole deformation parameters, defined as ϵ_4 , is such that the axial symmetry is preserved for oblate ($\gamma = \pm 60^\circ$) and prolate ($\gamma = 0^\circ$ and -120°)[115, 122] and the corresponding potential is given by $V_4(\gamma)$. The term V' contains the

anharmonic and spin-orbit coupling terms. The diagonalization of the above Hamiltonian generates single-particle energy values which are most often referred to as Routhians. As we have seen in earlier sections, the slope of the Routhian orbitals is proportional to alignment in $\langle j_x \rangle$, consequently, the orbitals with large values of $\langle j_x \rangle$ are strongly up or downsloping when Routhians are plotted as a function of cranking frequency. One such plot is shown in Fig. 5.14.

The CNS model is a pairing independent formalism. Thus, the model is effective for predicting high spin states where the pairing correlation is quenched. However, it was found that the results are also relevant in the intermediate- spin regime [123]. The unique feature of CNS is that the eigenfunctions of rotating harmonic oscillator [124] are used as basis states in single-particle diagonalization. Furthermore, each N_{rot} is divided into orbitals having their main amplitude in high- j intruder shells and in other low- j shells [125]. With this labelling of orbitals, configurations are fixed by the number of particles in groups characterized by (i) N_{rot} , (ii) high- j or low- j shells and (iii) signature quantum number. An energy scale based on mass excess is applied so that the calculated energies can directly be compared to the observed energies. The calculations minimize the energies for different configurations and for different spins with respect to the deformation parameters ϵ_2 , ϵ_4 and γ . The outcome of the calculations can be presented in various ways. The common way of analysis is to plot the excitation energy of a level relative to a rotating liquid drop as a function of spin. On the other hand, potential surface plots (PES) are useful to interpret the results in terms of deformation parameters. The PES plot deals with a stable prolate/oblate contour minimum in energy with respect to the deformation parameters. Routhians (as discussed above) are another mode of interpreting the results which highlights the occupancy of single-particle orbitals. Within the scope of the present thesis, all the calculations are done with κ and μ parameters for $A = 80$ [126]. The single-particle energies can also be plotted as a function of spin projections. The tilted Fermi

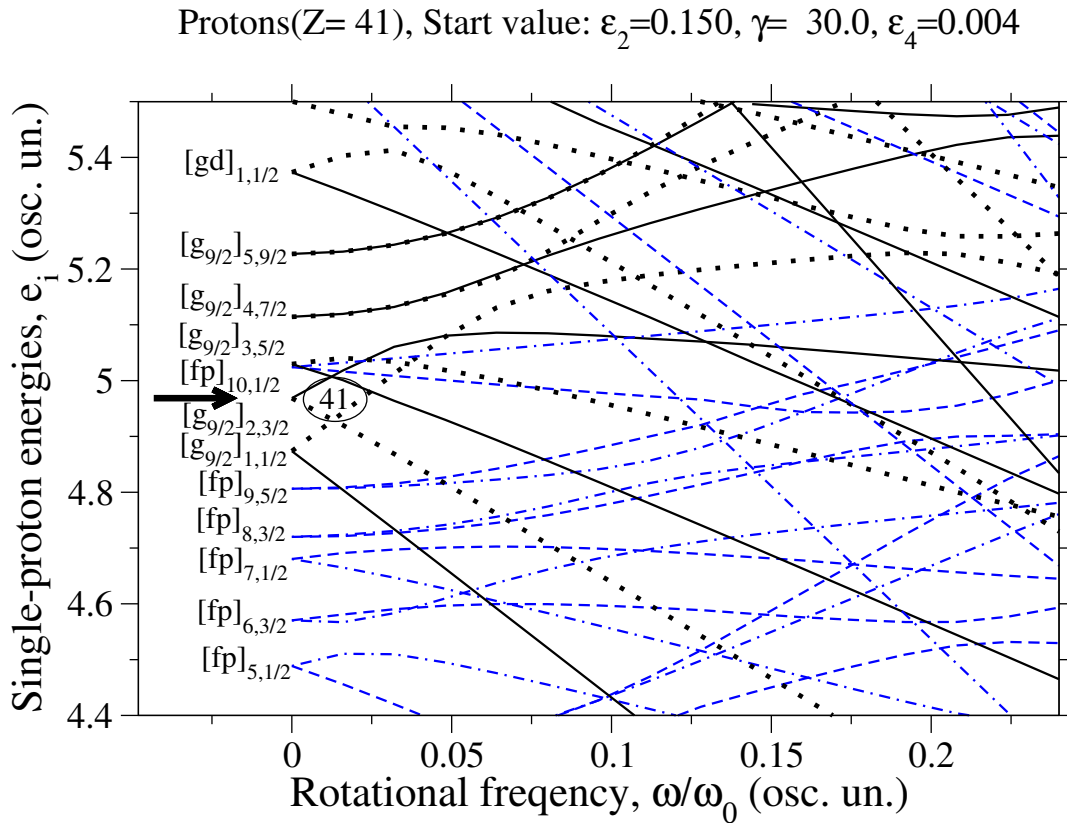


Figure 3.5 Single particle Routhians for protons typical triaxial deformation parameters $\varepsilon_2 = 0.15$, $\gamma = 30^\circ$ and $\varepsilon_4 = 0.004$. Four combinations of different (π, α) are plotted with the following representation: solid lines are for $(+, +1/2)$, dotted lines represent $(+, -1/2)$ whereas $(-, +1/2)$ and $(-, -1/2)$ are shown by dashed and dashed-dotted lines respectively. The labeling of the orbitals is done for zero rotational frequency. $[fp]$ and $[gd]$ represent the orbitals with dominant amplitudes in and $(p_{1/2}, p_{3/2}, f_{5/2})$ $(g_{7/2}, d_{5/2})$ respectively with the ordering and Ω -values as subscripts. The black thick arrow signifies the position of the Fermi level. For clarity the number of nucleons are mentioned at the zero rotational frequency. Figure taken from Ref. [111]. Details will be discussed in later sections.

surface method [110, 127] proves to be helpful in determining the optimal configurations across a terminating state. Several straight lines obeying the single particle vs spin projection rule for rotation about symmetry axis can be drawn corresponding to favored excited states outside the ^{93}Nb core (Discussed in Chapters 5).

3.4.4 Comparison of Experimental Data with Theoretical Calculations

There are several physical quantities which are used to compare the experimental observations with those of the calculated ones :

- Excitation energy, E_{exc} of a level relative to a rigid rotor reference, E_{rr} as a function of spin I [128] :

$$E_{rr} = \frac{1}{2J_{rig}} I(I+1) \quad (3.51)$$

where J_{rig} is determined by the relation $\frac{1}{2J_{rig}} \sim 32.32A^{-5/3} \text{ MeV}/\hbar^2$.

- Kinematic $J^{(1)}$ and dynamic $J^{(2)}$ moment of inertia as a function of angular frequency, ω .
- If lifetime measurement is possible, then the transitional quadrupole moment Q_t as a function of spin, I , is an effective tool for carrying out comparison between observed and model calculations.